Int. J. Electrochem. Sci., 16 **(2021)** Article ID: 210370, doi: 10.20964/2021.03.51

International Journal of
ELECTROCHEMICAL
SCIENCE
www.electrochemsci.org

Yeast derived Fe-doped Hollow Carbon as a Superior Sulfur Host for Li-S Batteries

Yifan Zheng, Wangjun Feng *

School of Science, Lanzhou University of Technology, Lanzhou 730050, China
*E-mail: wjfeng@lut.cn

Received: 23 November 2020 / *Accepted:* 13 January 2021 / *Published:* 31 January 2021

To overcome the charging and discharging problems of lithium sulfur batteries due to their shuttle effect, low conductivity, and volume expansion, researchers have proposed many solutions. Here, we designed an S@Fe-CY electrode in which yeast is carbonized at high temperatures to preserve its porous morphology, and then it is doped with Fe to enhance its electrochemical performance. The electrochemical test proved that S-@Fe-CY has excellent multiplication performance and cyclic stability. The initial discharge capacity of the lithium–sulfur battery with S@Fe-CY as the electrode material was 985.3 mAh/g at 0.2 C, which showed an improvement in electrochemical performance characteristics.

Keywords: Lithium-sulfur battery; porous carbon; thermal treatment

1. INTRODUCTION

At a time of vigorous development in all sectors of life, the demand for energy is increasing. Traditional lithium-ion batteries and electrochemical storage systems cannot meet the need of high-efficiency electrochemical storage systems. Compared with traditional lithium-ion batteries, lithium-sulfur batteries have a high specific capacity of up to 1675 mAh/g and specific energy of up to 2600 Wh/g, which are 3-5 times higher than those of commercial lithium-ion batteries. [1-3] In addition, as the positive electrode of batteries, sulfur materials are widely distributed and safe. Therefore, lithium-sulfur batteries are considered by researchers to be one of the most commercially promising batteries. [4-6] However, the development of lithium sulfur batteries has been hindered by some technical challenges. First, the insulation between the positive sulfur electrode and the final discharge product, Li_2S, greatly reduces the specific capacity of the positive electrode.[7] Second, a series of precipitation/dissolution reactions occur during battery charging and discharging, which results in the destruction of the positive electrode structure and a reduction in battery life.[8-9] Finally, in the discharge

intermediate product, polysulfide lithium easily dissolves in the electrolyte and directly reacts with the negative electrode to produce the "shuttle effect", which consumes the positive active substance and destroys the negative electrode, thus reducing the coulombic efficiency of the battery.[10-12]

To solve the above problems, the sulfur host in the positive electrode is improved, and the solubility of polysulfide lithium is reduced. Various strategies have been proposed, such as using carbon conductive skeletons [13-15] and polymer cladding [16] and adding nanometre-scale absorbents [17].

Currently, hollow carbon is the most popular material used to host sulfur due to its good physical adsorption of sulfur, and it can solve the “shuttle effect” of lithium-sulfur batteries. (18) As a method of fabricating porous carbon materials, high-temperature carbonation based on biological templates is effective. The hollow carbon material is directly carbonized through the complex structure of biological materials, which retains its original complex holes and provides the possibility for sulfur loading. [18-22]

As a common, safe and inexpensive material, yeast is a suitable biological template that can be used to produce porous carbon through carbonization very easily.[23] In addition, doping a certain amount of Fe at the same time makes it more conducive to the adsorption of sulfur on the material. Iron has a strong absorptivity and catalytic effect on lithium sulfide, which can effectively solve the abovementioned problems of lithium sulfur batteries.[24] Combined with carbon materials, the shuttle effect can be more effectively inhibited, and the reaction efficiency between positive and negative electrodes can be enhanced. [25]

In our work, yeast was used as a biological template and carbonized at high temperature to form the Yeast derived hollow carbon (CY) material. The CY material maintains the oval shape of yeast and is filled with holes of various shapes. In addition, to further improve the chemical adsorption of lithium sulfide by the positive electrode, we specifically doped iron into the CY material. In the final experiment, the positive electrode S@Fe-CY formed by the combination of the Yeast derived Fe-doped hollow carbon(Fe-CY) material and sulfur was found to have good electrochemical performance after the electrochemical test.

2. EXPERIMENT

2.1. Material preparation

The synthesis of Yeast derived hollow carbon (CY) has been discussed in previous research [24]. Yeast cells (3.0 g) were cultured in culture dishes at 35 ℃ for 0.5 h to form a uniform emulsion. Then, the uniform emulsion was obtained by centrifugation and washed several times with distilled water. After the whole culture process, to remove the lipids on the surface of the yeast cells, the obtained yeast cells were immersed in 40 mL acetone and continuously magnetically stirred for 12 h. After alternately washing with deionized water and ethanol, clean and available CY was obtained. Subsequently, the pretreated yeast cells and ferrous sulfate were mixed homogeneously and dispersed in 3% (v/v) ethylene glycol aqueous solution. The mixture was sealed within an 80 ml Teflon-lined autoclave and heated at 180 ℃ for 10 h. After the hydrothermal reaction, the red-brown product was washed with ethanol and

dried at 60 ℃ for 12 h. The red-brown product was first preheated at 300℃ for 6 h in air and finally at 800 ℃ for 10 h in an Ar atmosphere to form the Yeast derived Fe-doped hollow carbon (Fe-CY) composite.

2.2 Characterization

XRD patterns of all samples were obtained by a Bruker D8 Advanced diffractometer with Cu Kα radiation. The morphology and microstructure were examined on a JSM-6700F system and JEM-2100F systems operated at 20 kV and 200 kV.

2.3 Electrochemical Measurement

The slurry was composed of 0.24 g S@Fe-CY, 0.03 g super P, and 0.6 mL aqueous binder (LA133). The slurry was dispersed on aluminium foil and dried at 55 ℃ in a vacuum oven for 12 h. The electrochemical properties of the S@Fe-CY samples were detected by using CR-2025 coin-type cells. Galvanostatic charge-discharge cycling measurements were performed on a Land CT 2001A battery test system with a cut-off voltage window of 1.7-2.8 V. The electrolyte's volume was approximately 40 μL.

3. RESULTS AND DISCUSSION

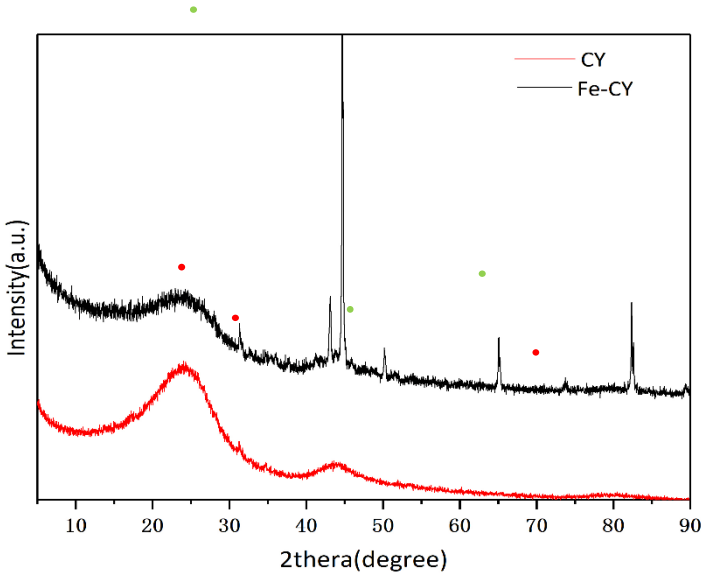

Figure 1. XRD patterns of the CY and Fe-CY materials

Figure 1 shows the XRD patterns of CY and Fe-CY. In Figure 1, the XRD pattern of CY shows peaks at 24° and 42° representing the diffraction peaks of carbon, and there are no other peaks; this indicates that there is only carbon in the CY material, and no other elements are doped in the material.

Moreover, the comparison is completely consistent with the original report, which further demonstrates successful synthesis. [24]

The CY material has a high carbon peak, which is even comparable to the carbon peak strength of carbon spheres and carbon nanotubes. This indicates that yeast has a high degree of carbonization after high temperature treatment and can obtain a good sulfur carrying performance. On the other hand, compared with carbon nanotubes and carbon spheres which are made of complex technology and expensive materials, the cheap and naturally porous morphology of yeast provides opportunities for the commercialization of CY materials. The single carbon material can only effectively undergo chemical adsorption to lithium sulfide, but the carbon material improved by adding Fe in our experiment can significantly increase the extent of chemical adsorption to lithium sulfide. The diffraction peaks indicated by the red dots in the XRD pattern of the Fe-CY material correspond to Fe atoms, and the diffraction peaks indicated by the green dots correspond to $CFe_{15.1}$. This indicates that iron ions are doped into the CY materials, which greatly improves the electrochemical performance of lithium sulfur cells made of CY materials.

$CFe_{1.5}$ provides sufficient active site for the adsorption and conversion of lithium sulfide, and the Fe atoms accelerate the REDOX reactions from the long-chain polysulfides to Li_2S_2/Li_2S. This has been proved by Zhang et al.[26] in their work of Ni-Fe Layered Double Hydroxide Hollow Polyhedrons through Fe atom doping to enhance the multiplier performance of the battery.

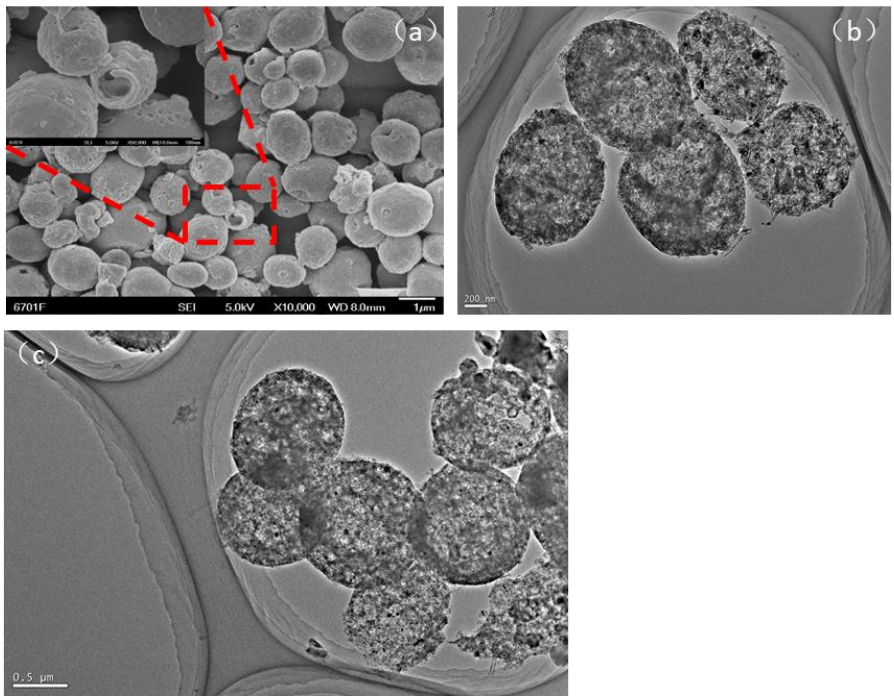

Figure 2. (a) SEM images of Fe-CY; (b-c) TEM images of Fe-CY;

Figure 2(a) shows the SEM images of Fe-CY. As seen from the SEM image, Fe-CY has a rough surface and many pores, which is conducive to fully adsorbing simple sulfur substances and provides

space for bulk expansion in the electrochemical reaction process to prevent the destruction of the positive sulfur poles. The Fe-CY material's ability to maintain its complete shape also indicates that the strong structure of yeast can maintain the structure of raw materials after they are carbonized at high temperature for a long time. This also implies that the Fe-CY material can withstand the damage caused by volume changes in the battery reaction process to ensure the electrochemical performance of the battery. First, compared with the chemically synthesized carbon sphere materials[27], CY materials have natural pores, and the number of pores varies. Second, different from the uniform size of carbon sphere material, CY material's size, which is controlled by yeast itself, is not uniform. The different sizes of CY materials make the space more fully filled and provide more active sites for lithium sulfide. As can be seen from the TEM image, within Fe-CY, there are many holes that are densely distributed and have large and small sizes. The Fe-CY material can fully absorb sulfur and ensure that enough binding sites are available for the electrode reaction to inhibit the occurrence of the shuttle effect in a timely manner.

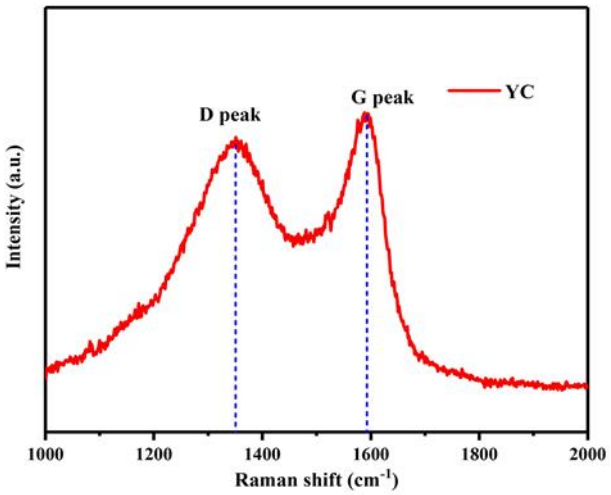

Figure 3. Raman spectrum of Fe-CY

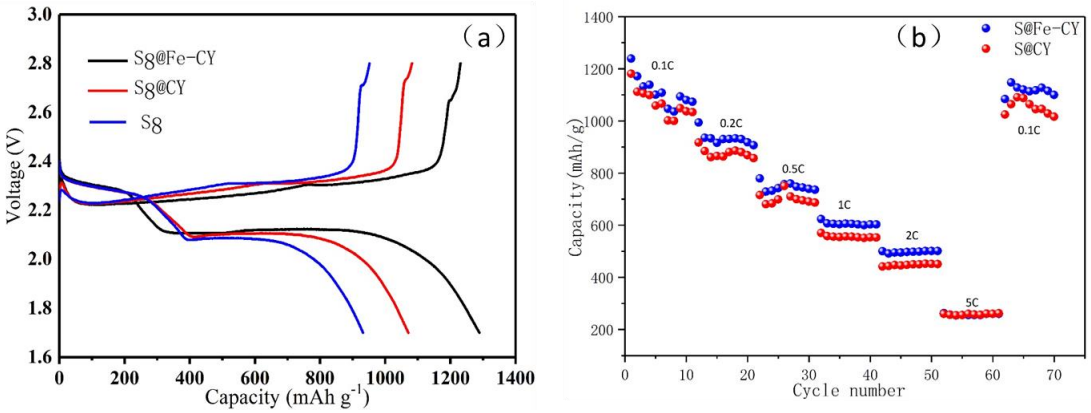

Figure 4. (a) Initial charge/discharge profiles of the S@Fe-CY, S@CY and S cathodes at 0.1 C. (b) Discharge profile of the specific capacity from 0.1 to 3 C after 10 cycles.

Raman spectroscopy was used to test the interaction between sulfur and CY and characterize the nature of CY materials/S (60 wt%). In Figure 3, we attributed the G peak at approximately 1580 cm^{-1} to the bond stretching vibration of graphitic carbon, whereas the D-band at approximately 1350 cm^{-1} is ascribed to disorder, edges and defects. The Raman intensity ratio of the D-band to the G-band (I_D/I_G) is approximately 0.75, which indicates a partial graphitic content, which facilitates the transfer of electrons from sulfur, a poor conductor.

Figure 4(a) shows the initial charge/discharge profiles of CY@S and Fe-CY@S at 0.1 C. There were two plateaus in the discharge process. The first discharge plateau observed at 2.3 V-2.1 V was attributed to the reduction of long-chain Li_2S_8 to short-chain lithium polysulfides (Li2Sn, $4 \leq n < 8$). The second plateau, which is longer than the first, was attributed to the reduction from soluble Li_2S_n to insoluble Li_2S_2 and Li_2S. The first initial discharge capacities of S@Fe-CY and S@CY were 1285 mAh/g and 1094 mAh/g, respectively; the initial discharge capacity of S@Fe-CY was significantly higher than that of S@CY, which indicates that S@Fe-CY has better multiplicity capacity than S@CY, indicating that the iron mixed in CY is capable of catalytic reactions. The reaction rate of lithium sulfide is accelerated. The first initial discharge capacity of the S electrode is 932 mAh/g, which is far less than the discharge capacity of the S@CY electrode, which indicates that the CY material speeds up the reaction rate of the battery and that carbonized yeast enhances the reaction efficiency of the electrode. The original pores of yeast provide a large reaction area for sulfur-containing substances.

Figure 4(b) shows the discharge rate of the specific capacity from 0.1 to 3 C after 10 cycles. Clearly, the S@Fe-CY material capacity is always higher than that of the S@CY material, which further verifies the conclusion of Figure 4a. In addition, for a cycle performed at a current lower than 0.1 C, the capacity attenuation of the S@Fe-CY electrode within ten cycles is not large, indicating that the participation of carbonized yeast and iron reduces the damage of the positive electrode, impedes the dissolution of lithium sulfide, and slows down the shuttle effect.

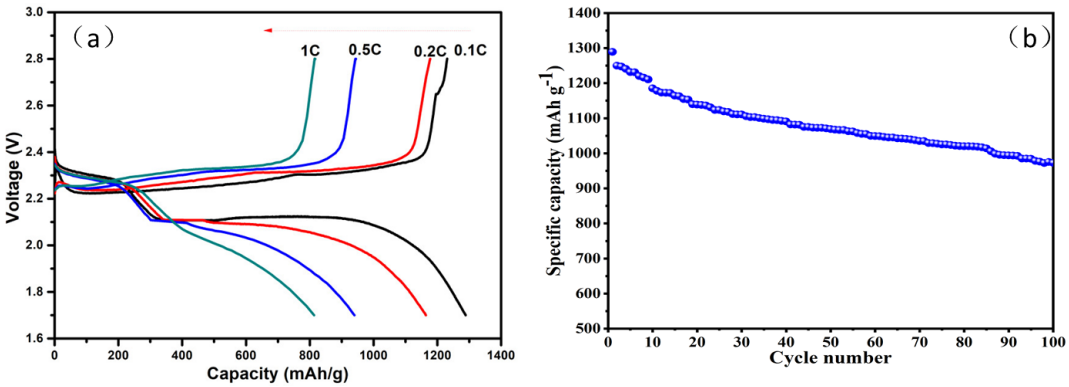

Figure 5. (a) First charge/discharge profiles of S@Fe-CY, CY@S and Fe-CY@S at 0.1 C-3 C. (b) Cyclic stability of S@Fe-CY cathodes at a current of 0.2 C.

In addition, under the condition of the first cycle at 0.1 C, the average capacity of the ten cycles of the S@Fe-CY material is 1100 mAh/g. After the current is gradually strengthened and cycled 50 times, the current decreases again to 0.1 C, with an average capacity of 1085 mAh/g, which is almost the same as the capacity after the first cycle. This indicates that the structure of the S@Fe-CY electrode

can remain intact after high-current impact, and the cell efficiency is not affected. The results showed that the carbonized yeast material had strong resistance to electric current.

Figure 5(a) shows the first charge/discharge profiles of S@Fe-CY at 0.1 C-2 C. At 0.1 C, the initial discharge capacities at 0.1 C, 0.2 C, 0.5 C, and 1 C were 823.5, 954.3, 1185.5, and 1303.3 mAh/g, respectively. After the cycling of the S@Fe-CY material, the discharge curve still maintains two plateaus, which further indicates that the electrode has a good structure and that the battery reaction remains intact after multiple cycles.

Figure 5(b) studies the cycling stability of S@Fe-CY cathodes at a current of 0.2 C. The first discharge capacity of the electrode is 1284.3 mAh/g; after 100 cycles, and the electrode capacity is 995.3 mAh/g. Compared with that of the cathode of a common lithium sulfur battery, the capacity of the electrode is much higher, which indicates that the material has good performance as the carrier of a lithium sulfur battery anode material.

Table 1. Comparison with other currently reported carbon materials

Carbon source	Price	Cycling performance at 0.2C after 50 cycles	Reference
aqueous ammonia	very expensive	900 mA/g	[7]
Metal organic framework	expensive	999.69 mA/g	[8]
yeast	cheap	1073.4mA/g	this work

By comparison with other materials showed in table 1, it can be seen that yeast has the characteristics of low price, an obvious advantage of commercialization. In addition, a yeast material cycle performance is the highest due to its unique morphology structure, and the added iron atoms into the lithium sulfide provides enough rich active sites for its adsorption and transformation and greatly accelerates the charge-discharge reaction kinetics of the process, thus ensure the stability of the anode structure. In summary, CY material obtained from yeast as carbon source is used as sulfur carrier material to form uniform positive electrode material that facilitates the insertion and extraction of lithium ions.

4. CONCLUSION

Commercial yeast is directly transformed into CY by the high-temperature carbonization method, and Fe-CY is obtained by Fe doping. As a carrier of sulfur electrodes, this material can effectively

improve the battery ratio and cycling stability. SEM and TEM showed that the Fe-CY material has a porous and complex structure. These holes can fully load S and effectively alleviate the bulk expansion effect in the charging and discharging process of the electrode. In addition, the electrode reaction efficiency can be further enhanced through the interaction between lithium sulfide and Fe. To summarize the results obtained in this study, this high-temperature carbonized CY material can be used as a host of sulfur electrodes for high-efficiency lithium sulfur batteries, which has been proven by electrochemical tests.

FUNDING INFORMATION
This work was financially supported by the National Natural Science Foundation of China (Grant No. 21965019).

Reference

1. M. Li, W. Feng, X. Wang, *Journal of Alloys and Compounds*, 853 (2021) 157194
2. G. Gao, W. Feng, W. Su , S. Wang, L Chen, M Li, C Song ,*Int. J. Electrochem. Sci*., 15(2020)1426-1436
3. Y. Zheng, W. Feng, L. Chen, *Int. J. Electrochem. Sci*., 15(2020) 8527–8535.
4. S. Tu, X. Chen, X. Zhao, M. Cheng, P. Xiong, Y. He, Q. Zhang, Y. Xu, *Adv. Mater*., 30 (2018) 1804581.
5. H. Tang, W. Li, L. Pan, K. Tu, F. Du, T. Qiu, J. Yang, C.P. Cullen, N. McEvoy, C. (John) Zhang, *Adv. Funct. Mater*., 29 (2019) 1901907.
6. 6.D. Liu, C. Zhang, G. Zhou, W. Lv, G. Ling, L. Zhi, Q.-H. Yang, *Adv. Sci.,* 5 (2018) 1700270.
7. J.-Y. Hong, Y. Jung, K.-M. Kim, S. Kim, *J Nanosci Nanotechnol*, 18 (2018) 279–283.
8. K. Zhang, Q. Zhao, Z. Tao, J. Chen, *Nano Res*., 6 (2013) 38–46.
9. D. Gueon, M.-Y. Ju, J.H. Moon, *Proc Natl Acad Sci USA*, 117 (2020) 12686–12692.
10. C. Li, X. Liu, L. Zhu, R. Huang, M. Zhao, L. Xu, Y. Qian, *Chem. Mater*., 30 (2018) 6969–6977.
11. X. Chen, S. Zeng, H. Muheiyati, Y. Zhai, C. Li, X. Ding, L. Wang, D. Wang, L. Xu, Y. He, Y. Qian, *ACS Energy Lett*., 4 (2019) 1496–1504.
12. T. Gao, T. Le, Y. Yang, Z. Yu, Z. Huang, F. Kang, *Materials*, 10 (2017) 376.
13. W. Yang, W. Yang, L. Dong, X. Gao, G. Wang, G. Shao, *J. Mater. Chem*. A, 7 (2019) 13103–13112.
14. D. Wang, Y. Yu, W. Zhou, H. Chen, F.J. DiSalvo, D.A. Muller, H.D. Abruña, *Phys. Chem. Chem. Phys.*, 15 (2013) 9051.
15. G. Zhou, E. Paek, G.S. Hwang, A. Manthiram, *Nat Commun,* 6 (2015) 7760.
16. Y. He, L. Xu, C. Li, X. Chen, G. Xu, X. Jiao, *Nano Res*., 11 (2018) 3555–3566.
17. Z. Wang, J. Shen, J. Liu, X. Xu, Z. Liu, R. Hu, L. Yang, Y. Feng, J. Liu, Z. Shi, L. Ouyang, Y. Yu, M. Zhu, *Adv. Mater*., 31 (2019) 1902228.
18. S. Wang, W.-C. Li, G.-P. Hao, Y. Hao, Q. Sun, X.-Q. Zhang, A.-H. Lu, *J. Am. Chem. Soc*., 133 (2011) 15304–15307.
19. M.R. Cerón, M. Izquierdo, N. Alegret, J.A. Valdez, A. Rodríguez-Fortea, M.M. Olmstead, A.L. Balch, J.M. Poblet, L. Echegoyen, *Chem. Commun*., 52 (2016) 64–67.
20. S. Yang, X. Feng, L. Zhi, Q. Cao, J. Maier, K. Müllen, *Adv. Mater*., 22 (2010) 838–842.
21. G. Zheng, S.W. Lee, Z. Liang, H.-W. Lee, K. Yan, H. Yao, H. Wang, W. Li, S. Chu, Y. Cui, *Nature Nanotech*, 9 (2014) 618–623.
22. G. Zhou, Y. Zhao, A. Manthiram, *Adv. Energy Mater*., 5 (2015) 1402263.
23. S. Shen, X. Xia, Y. Zhong, S. Deng, D. Xie, B. Liu, Y. Zhang, G. Pan, X. Wang, J. Tu, *Adv. Mater*.,

31 (2019) 1900009.
24. J. Zhang, Z. Li, Y. Chen, S. Gao, X.W.D. Lou, *Angew. Chem*., 130 (2018) 11110–11114.
25. X. Tao, J. Zhang, Y. Xia, H. Huang, J. Du, H. Xiao, W. Zhang, Y. Gan, *J. Mater. Chem*. A, 2 (2014) 2290–2296.
26. J. Zhang, Z. Li, Y. Chen, S. Gao, X.W.D. Lou, *Angew. Chem. Int. Ed*., 57 (2018) 10944–10948.
27. K. Zhang, Q. Zhao, Z. Tao, J. Chen, *Nano Res*., 6 (2013) 38–46.